3

Navigating Autonomous Underwater Vehicles

Brian Bingham
Franklin W. Olin College of Engineering
U.S.A

Navigation is the process of directing the movements of a ship or aircraft form one point to another. Both art and science are involved in conducting a ship safely to its destination.

(Dunlap, 1975)

1. Introduction

Autonomous Underwater Vehicles (AUVs) are powerful tools for exploring, investigating and managing our ocean resources. As the capabilities of these platforms continue to expand and they continue to mature as operational assets, navigation remains a fundamental technological component.

This chapter presents a road map for the vehicle designer to aid in integrating the latest navigation methods into new platforms for science, industry and military platforms. Along the way, we point to emerging needs where new research can lead directly to an expansion of the operational abilities of these powerful tools. To accomplish this we start by describing the problem, explaining the needs of vehicle users and the challenges of autonomous localization. Next we explain the state of practice, how operational assets currently solve this difficult problem. To expand this explanation we present new research targeted at helping AUV builders to make the complex tradeoffs in creating a platform with the appropriate navigation solution. We conclude with an overview of the latest research and how these advances might soon become available for AUV operations in new environments such as the littoral zone, at the poles and under-ice. Throughout this chapter we attempt to reach across the disciplinary boundaries that separate the researcher from the operator.

2. Motivation

2.1 The challenge of autonomous underwater navigation

Navigating an AUV presents unique challenges to the researcher and the practitioner. One way to understand the particularities of this challenge is to consider two important facets of AUV operations: the marine environment and desired results.

The ocean environment presents both challenges and opportunities for autonomous navigation. The challenges are well documented: seawater is opaque to electromagnetic signals making Global Positioning System (GPS) solutions infeasible; acoustic communication

Source: Underwater Vehicles, Book edited by: Alexander V. Inzartsev,
ISBN 978-953-7619-49-7, pp. 582, December 2008, I-Tech, Vienna, Austria

is limited in bandwidth, scale and reliability (Catipovic, 1990) and the ocean environment is observationally limited and ever-changing.
On the other hand the deep-sea environment can be an ideal place for autonomous vehicle operations. The unstructured environment can be structured by the addition of acoustic transponders moored to the seafloor or through close communication with a surface ship. Either method provides an absolute position reference which decreases the demands on real-time perception and decision making. Also, deep-water can be one of the most forgiving acoustic environments because of the homogeneous and stable sounds speed structure and low ambient noise.
The opportunity for novel observation counterbalances these operational difficulties. We have better maps of Mars, Venus and the Moon that we have of the Earth's ocean, creating a great potential to advance our observational capability through technology.

2.2 Creating new data products

Typically a gap between the needs of the AUV user and the capabilities of the navigation solution. The user is often not directly interested in the navigation, but instead is focused on producing a *data product*, an gestalt representation of the underwater environment. The vehicle designer should incorporate the right navigation instruments and the right data processing to provide a navigation solution appropriate for the desired data product. This perspective, having the requirements of the data product drive the design decisions, leads to closing the gap illustrated in Fig. 2.

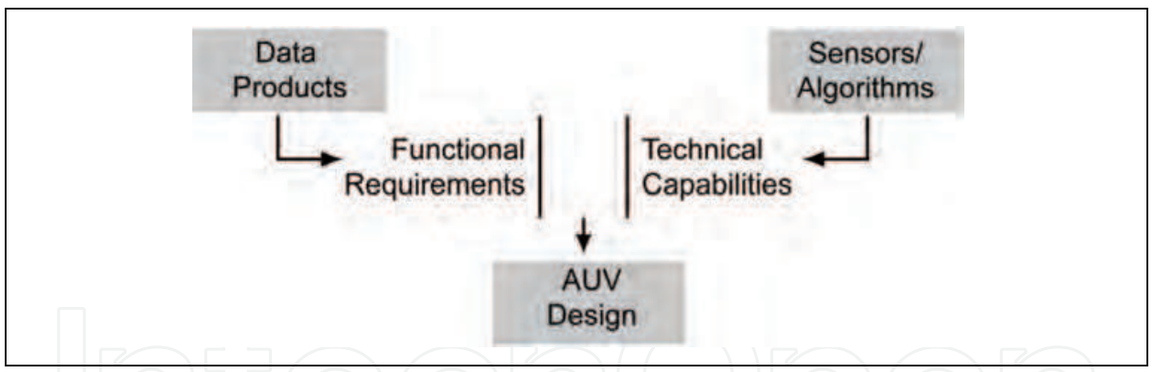

Fig. 1. Illustration of how vehicle design decisions are driven by the needs of the application (the desired data product) and the capabilities of the navigation sensors and algorithms.

It is only a slight over simplification to consider the resolution of any observation to be directly proportional to the navigation precision. Fig. 2 shows a common situation to illustrate this notion. In this case the data products are a photomosaic and a small-scale bathymetry map, both shown in the figure. The remotely operated vehicle (ROV) JASON is shown as it surveys the seafloor. Navigation allows all the measurements (e.g., sonar bathymetry) and observations (e.g., optical images) to be placed in a common coordinate system. How well we can resolve two disparate data sources, i.e., the resolution of our data product, depends on the uncertainty in our navigation. Summarized another way, the spatial size of each "pixel" in our final image is fundametnally limited to the uncertainty in our navigation solution.

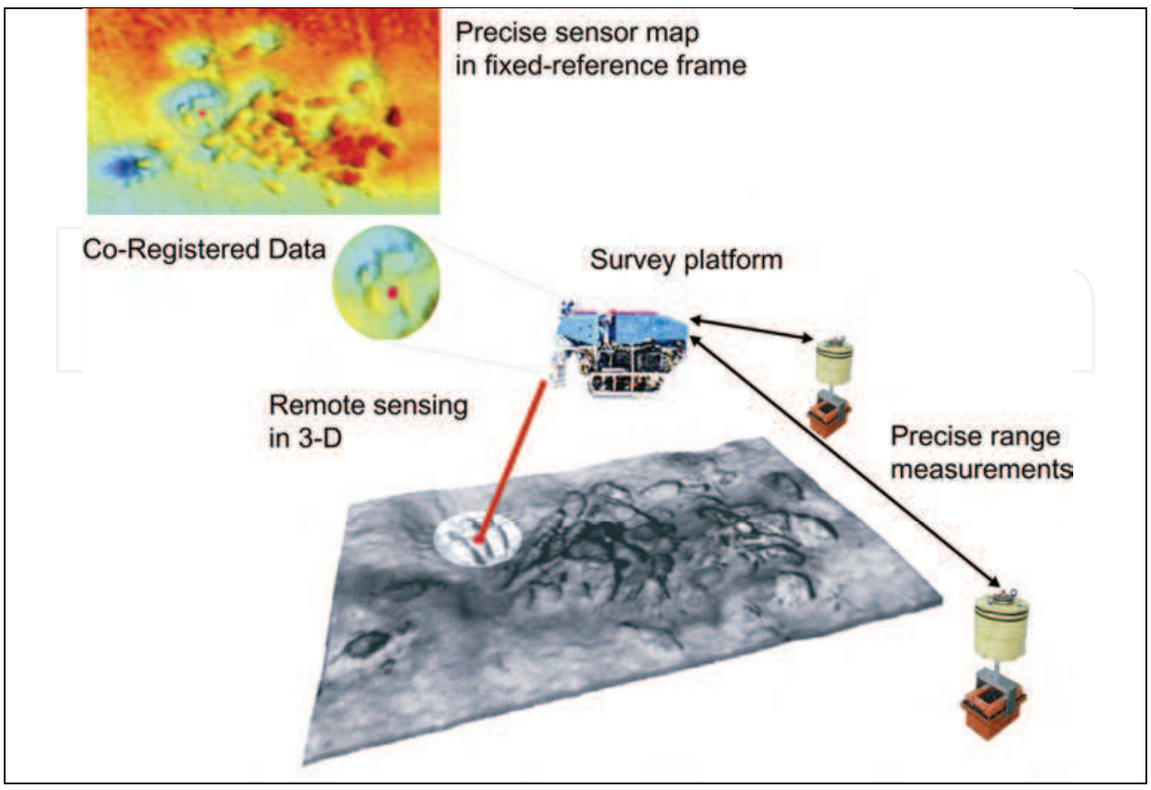

Fig. 2. Illustration of the concept of co-registered data. The ROV JASON is shown performing a survey collecting optical images and bathymetry data. Range-based navigation provides a common coordinate system. Component images are courtesy of the Deep Submergence Lab (DSL) at the Woods Hole Oceanographic Institution.

3. State of practice

AUV operations require a reliable navigation solution. Methods currently in operation on autonomous platforms are simple and robust. These real-world solutions typically make use of just a few key sensors:

- GPS receivers to measure position at the surface
- Long baseline transponders to measure the distance from the AUV to transponders in known locations.
- Doppler velocity logs to measure velocity relative to the bottom, supported by attitude and heading measurements

These sensors are dedicated navigation sensors, distinct from the remote sensing payload sensors which collect measurements which are not processed for real-time perception. These relatively simple sensing modalities, configured and combined in a variety of interesting ways, have proven to provide a variety of solutions that are robust to the complexities of the ocean environment.

3.1 An example

It is informative to consider a particular example. This example, like the data shown in Fig. 2, is taken from work with the JASON ROV system from the Deep Submergence Lab at

Woods Hole Oceanographic. The ROV is instrumented with a combination that has become standard in AUV and ROV applications: absolute positioning using LBL transponders and seafloor odometry from a DVL and heading reference.

To understand the tradeoffs in designing an appropriate navigation system it is useful to contrast modalities that exhibit unbounded error growth with those that have bounded error. Fig. 3 illustrates this contrast. The dead-reckoning solution provided by the DVL alone is shown to drift over time; the error growth is unbounded. In Fig. 3 the DVL track begins at the origin (shown in the figure as a large "X") and then diverges from the absolute reference provided by the LBL reference. In what follows we show how quantitative models of this error accumulation can be used to improve design and operation.

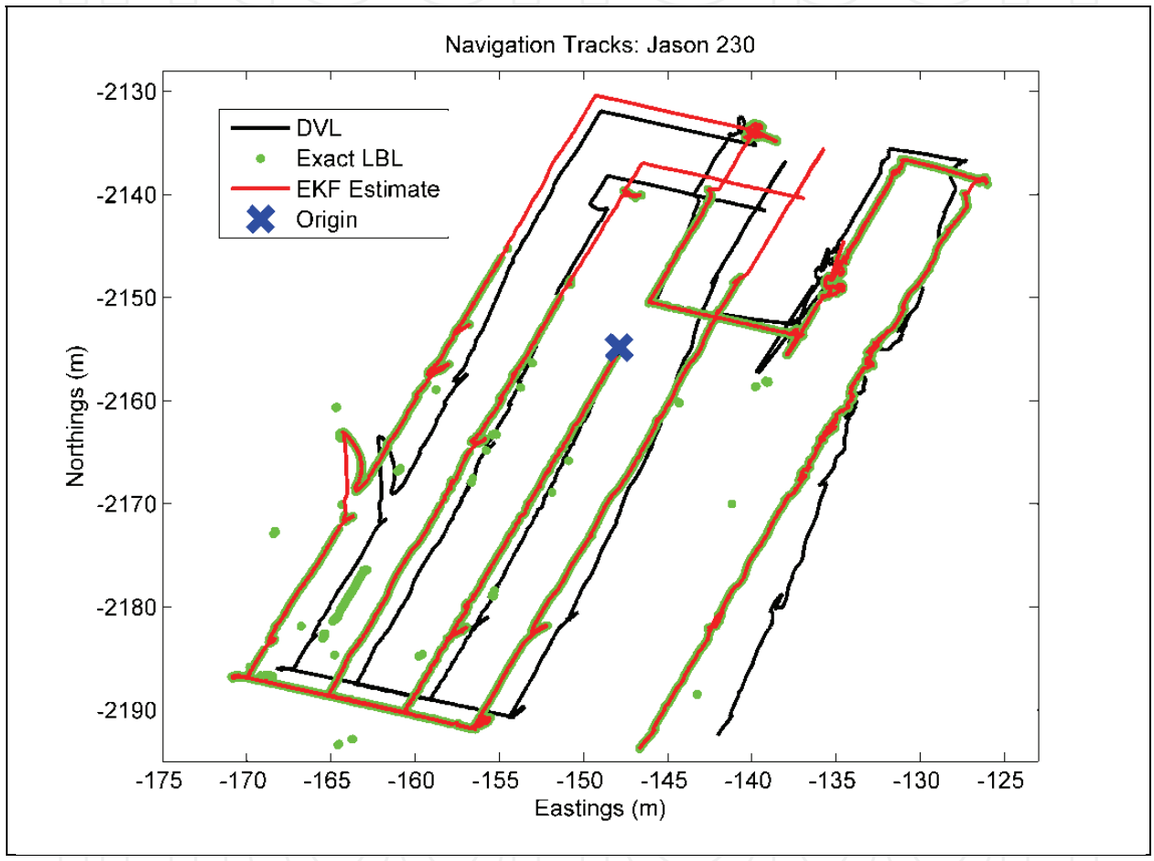

Fig. 3. Three navigation tracks from the ROV Jason, lowering #230. The "DVL" track shows the dead-reckoning resulting from the DVL odometry alone. The "Exact LBL" track shows the standalone LBL solution. The "EKF Estimate" track shows the combination of both the DVL and LBL information using an extended Kalman filter framework. All tracks are started at the "Origin". The tracklines were executed over 3.5 hours at an average depth of 2,265 m.

The LBL position solution complements the DVL dead-reckoning. Returning to Fig. 3 we see that the Exact LBL provides a solution with bounded uncertainty, but with a high degree of random errors or noise. We can see outliers (shown by widely spaced data points) and zones where no LBL is returns are received (eg., the Exact LBL track dissappears in the northwest corner of the figure). A particularly insidious form of error is the consistent, but

off-set position solutions shown in the southwest section of the survey. This type of error can be difficult to filter autonomously.

Finally, to illustrate the possibility of leveraging the complementary nature of the two navigation tracks, we show the results of an extended Kalman filter (EKF) estimator. This track uses absolute positioning from the LBL source to constrain the unbounded uncertainty in the DVL dead-reckoning. By simultaneously using both sources of information, the EKF solution combines the strengths of both methods. This example highlights the contrasts between the unbounded uncertainty of DVL dead-reckoning, the bounded uncertainty of LBL positioning and the utility of combining these two solutions.

3.2 Long Baseline (LBL) positioning

Long baseline (LBL) positioning is a standard in underwater navigation. First used in the 1960's and 1970's (Hunt, Marquet, Moller, Peal, Smith, & Spindel, 1974), the foundational idea of using acoustic transponders moored to the seafloor has been used to fix the position of a wide spectrum underwater assets: submersibles, towed instrumentation, ROVs and AUVs. Fig. 4 illustrates the basic LBL method for use with an AUV. For each navigation cycle the vehicle measures the two-way time-of-flight for an acoustic signal sent round trip between the platform and fixed transponders on the seafloor. Position is determined by multilateration, typically implemented as a non-linear least-squares solution to the spherical positioning equations.

Due to the particular challenges and constraints of working in marine environments, a large variety of range-based positioning solutions have been put into practice. The ability to precisely measure the range between two acoustic nodes is the foundation of any such solution. For example, short baseline (SBL) techniques are equivalent to the LBL positioning except that the transponders are in closer proximity, often mounted to the surface ship or platform (Milne, 1983) (Smith & Kronen, 1997). Wired configurations are used in small environments and allow one-way range measurement (Bingham, Mindell, Wilcox, & Bowen, 2006). Such solutions can be particularly useful for confined environments such as small test tank (Kinsey, Smallwood, & Whitcomb, 2003).

There are many implementations of the basic LBL positioning method. Commerical systems are available to provide support for scientific, military and industry application. Typical systems operate at frequencies near 10 kHz with maximum ranges of 5-10 km and range resolution between 0.5 and 3 m[1]. Specific purpose systems are also available for small-scale high-resoution positioning[2] or even subsea geodetics.

Fig. 5 is a conceptual sketch of the method of spherical positioning which can be generalized with a stochastic measurement model. Each spherical positioning solution is based on observing individual range values (z_{r_i}) between known fixed beacon locations ($\boldsymbol{x}_{b_i}$) and an unknown mobile host position ($\boldsymbol{x}_h$) where the individual range measurements is indexed by i.

$$z_{r_i} = \left|\boldsymbol{x}_h - \boldsymbol{x}_{b_i}\right| + \omega_{r_i} \tag{1}$$

We consider the additive noise in each measurement (ω_{r_i}) as an independent, zero-mean, Gaussian variable with variance σ_r^2.

[1] Examples include solutions from Teledyne Benthos, Sonardyne International Ltd. and LinkQuest Inc.

[2] Examples include solutions from Desert Star Systems or Marine Sonics Technology, Ltd.

$$\omega_{r_i} \sim \mathcal{N}(0, \sigma_r^2) \quad (2)$$

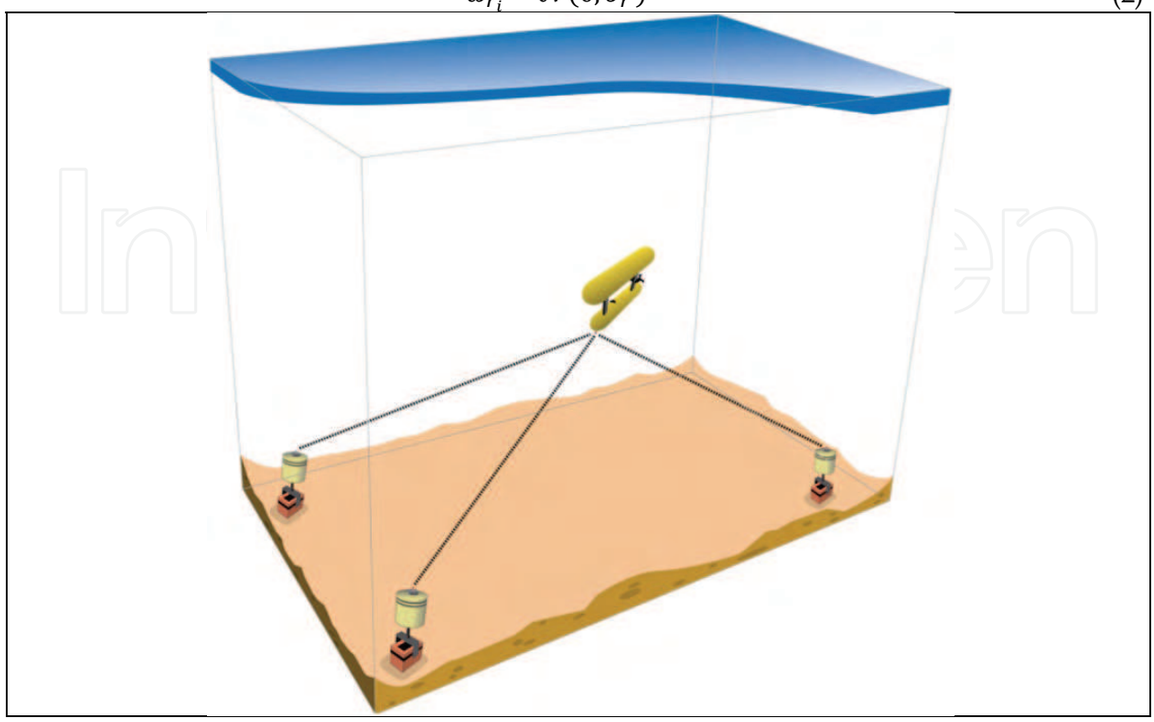

Fig. 4. Illustration of long baseline (LBL) positioning of an AUV in an instrumented environment. Three transponders are shown moored to the seafloor. Three time-of-flight range observations are represented by dashed lines between the seafloor transponders and the mobile host, in this case an autonomous underwater vehicle.

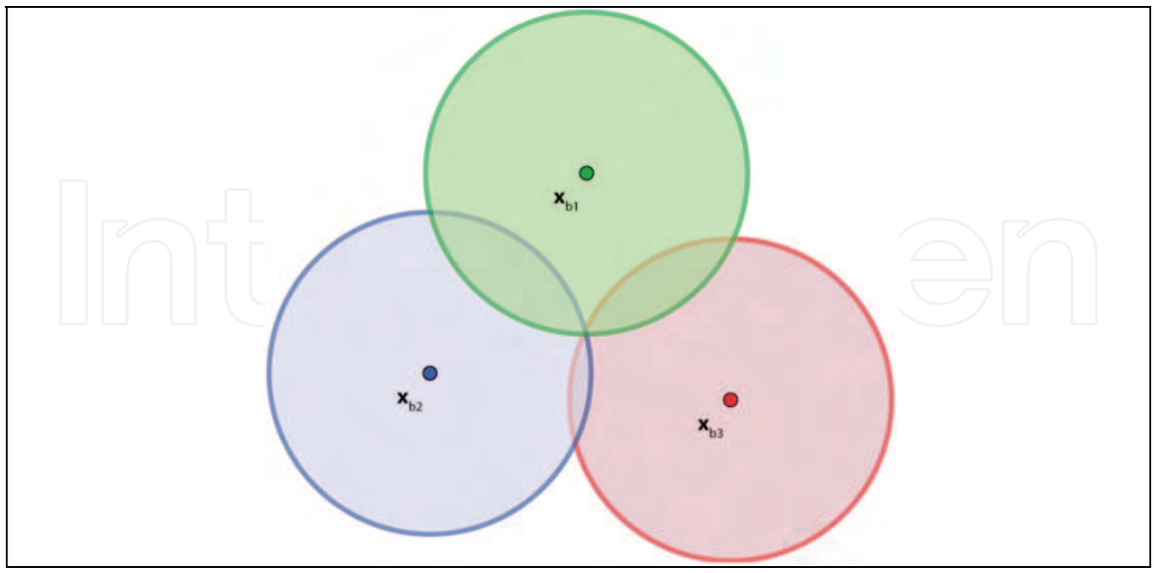

Fig. 5. Illustration of a standalone spherical positioning solution, shown in two dimensions. Each of the three transponders is represented by a mark at the center of the three circles

(x_{b_i}). By measuring a range from each transponder we know the radius of each circle. With three ranges the position is estimated by the intersection of the three circles.

3.3 Doppler Velocity Log (DVL) dead-reckoning

A Doppler velocity log (DVL), integrated with a precise heading reference, is another standard instrument for underwater robotics. As a standalone solution, DVL navigation provides a dead-reckoning estimate of position based on discrete measurements of velocity over the seafloor. To produce this dead-reckoning estimate in local coordinates sequential DVL measurements are related to a common coordinate system. Because the raw measurements are made relative to the sensor, the attitude (heading, pitch and roll) of the sensor relative to the common coordinate system must be measured. Once compensated for attitude, the velocity measurements are accumulated to estimate position.

The position uncertainty for standalone DVL dead-reckoning grows with both time and distance. Fig. 6 illustrates a simple example of this error growth based on a vehicle moving at a constant speed along the x-axis. Velocity uncertainty causes uniform error growth in both directions while heading uncertainty dominates the error growth in the across track direction. To further quantify the dynamics of uncertainty in such a situation we propose an observation model compatible with the LBL uncertainty model presented above.

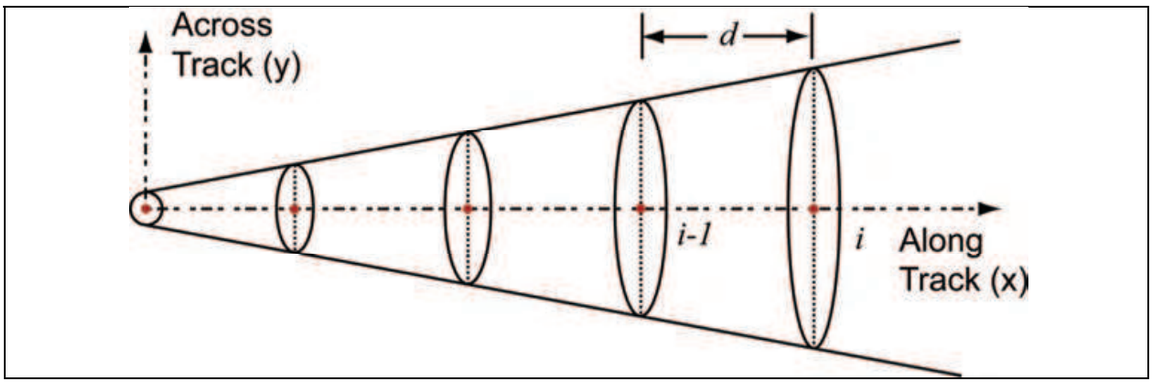

Fig. 6. Illustration of odometry uncertainty dynamics. The ellipses illustrate the 1-σ uncertainty in the along track (x) and across track (y) directions. Five discrete vehicle positions are shown, indexed by i. The distance between consecutive positions is indicated by d.

The DVL instrument provides independent measurements of velocity (z_{v_k}) in each of three dimensions (indexed by k).

$$z_{v_k} = v_k + \omega_{v_k} \tag{3}$$

We characterize the uncertainty as mutually independent additive, zero-mean, Gaussian white noise.

$$\omega_{v_k} \sim \mathcal{N}(0, \sigma_{v_k}^2) \tag{4}$$

Transforming these sensor frame measurements into a local coordinate frame requires knowledge about sensor and vehicle attitude. Heading is the most important and difficult to accurately observe measurement for this coordinate rotation. Again we use a simple additive Gaussian noise model to represent the heading (ψ) measurement.

$$z_\psi = \psi + \omega_\psi \tag{5}$$

$$\omega_\psi \sim \mathcal{N}(0, \sigma_\psi^2) \tag{6}$$

It is possible to carry forward the complete three dimensional ($k = \{1,2,3\}$) formulation (Eustice, Whitcomb, Singh, & Grund, 2007), but it is non-limiting to simplify this representation to a two dimensional representation. In particular we assume the pitch and roll are transformations that do not affect the uncertainty growth. We also consider the uncertainty along-track to be independent of the uncertainty across track. These considerations capture the dominant dynamics of error growth (velocity and heading uncertainty) and allow us to simplify our two-dimensional model, preserving intuition. The resulting odometry measurement model considers discrete observations of incremental distance ($\boldsymbol{z}_{o_j}$), where j is the temporal index for sequential velocity measurements.

$$\boldsymbol{z}_{o_j} = (\boldsymbol{x}_{h_j} - \boldsymbol{x}_{h_{j-1}}) + \boldsymbol{\omega}_o \tag{7}$$

The additive noise is characterized by a two-dimensional covariance matrix ($\boldsymbol{\Sigma}_o$) in the along track and across track directions.

$$\boldsymbol{\omega}_o \sim \mathcal{N}(0, \boldsymbol{\Sigma}_o) \tag{8}$$

$$\boldsymbol{\Sigma}_o = \begin{bmatrix} t\sigma_v^2 & 0 \\ 0 & d^2\sigma_\psi^2 \end{bmatrix} \tag{9}$$

The diagonal matrix in equation (9) is a consequence of the independent along track and across track uncertainty growth. The along track term, in the upper left, captures growth of position uncertainty as a function of velocity uncertainty, based on random walk uncertainty growth. The across track term, in the lower right, is dominated by heading uncertainty; therefore, the across track uncertainty grows linearly with distance travelled.
Returning to Fig. 6 we can predict how the odometry error will grow for a straight line vehicle trajectory. The figure shows the along track uncertainty the x direction and across track uncertainty in the y direction. The aspect ratio of error ellipses increases with time, illustrating combination of linear growth of the along track uncertainty (growing with distance travelled) and growth proportional to the square root of time of the along track position.

3.4 Data fusion

These two standalone navigation solution, LBL positioning and DVL dead-reckoning, are a complementary pair of information sources. Fusing these sources can exploit both the precision of the DVL solution and the accuracy of the LBL reference. The introduction to this section provided a qualitative discussion of this integration, and there are many excellent references with the details of how to combine these two sensing modalities.
(Whitcomb, Yoerger, & Singh, 1999) (Larsen M. B., 2000).

4. Tradeoffs in designing navigation solutions

How does the vehicle designer decide which navigation solutions to employ and how to configure them? This section describes a framework for making these decisions based on

applications of estimation theory to the problem of estimating position based on noisy measurements. This model enables designers to predict the performance of candidate designs based on their quantitative performance metrics. Using this analysis framework we present the answer to particular questions often asked when designing and deploying a range-based positioning system:

- What is the "best" geometry of the fixed acoustic nodes and mobile nodes in an LBL network? What is the sensitivity of the system precision with respect to changes in this geometry?
- What is the relative importance of geometry vis-á-vis range precision in an LBL network?
- What is the best range-based configuration (geometry and update rate) to integrate with dead-reckoning solutions.

To quantify these tradeoffs we propose metrics for positioning precision based on standard terrestrial positioning problems. We use the Cramér Rao lower bound (CRLB) to frame the question in a way that affords thorough analysis. Based on this framework, we articulate particular design tradeoffs, e.g., how design choices affect precision of the position estimate.

4.1 Analytical framework for predicting performance

Navigation is an estimation problem; a set of unknown parameters, location and attitude, are estimated from a set of observations. The CRLB is a standard tool for determining the uncertainty in the estimate based on uncertainty in the observations and a model relating the observed and estimated quantities.

Consider the estimation of an unknown parameter vector $\boldsymbol{x}$ from a set of observations $\boldsymbol{z}$ with known probability density $p_{\boldsymbol{z}}(\boldsymbol{z};\boldsymbol{x})$. An estimator extracts the information from these observations to derive and estimate of the parameters based on the measurements, $\hat{\boldsymbol{x}}(\boldsymbol{z})$. The uncertainty in this estimate is a direct consequence of how much information is available from the measurements. When it exists, the CRLB gives the lower bound on the variance of *any* valid unbiased estimator (Bar-Shalom, Li, & Kirubarajan, 2001). The *Fisher information*, $\boldsymbol{I}_{\boldsymbol{z}}(\boldsymbol{x})$ is the information about the parameters, $\boldsymbol{x}$ contained in the observations, $\boldsymbol{z}$.

$$\boldsymbol{I}_{\boldsymbol{z}}(\boldsymbol{x}) = E\left[\frac{\delta^2}{\delta x^2}\ln p_{\boldsymbol{z}}(\boldsymbol{z};\boldsymbol{x})\right]\boldsymbol{z}_{o_j} = (\boldsymbol{x}_{h_j} - \boldsymbol{x}_{h_{j-1}}) + \boldsymbol{\omega}_o \tag{10}$$

Where $E[\ \ ]$ is the expectation operator. The CRLB, $\boldsymbol{\Lambda}(\hat{\boldsymbol{x}}(\boldsymbol{z}))$, is the inverse of the Fisher information, i.e.,

$$\boldsymbol{\Lambda}\big(\hat{\boldsymbol{x}}(\boldsymbol{z})\big) = [\boldsymbol{I}_{\boldsymbol{z}}(\boldsymbol{x})]^{-1} \tag{11}$$

The CRLB is the minimum uncertainty achievable by an unknown optimal estimator. An estimator that approaches this existence of the lower bound is *efficient*, but the bound does not guarantee that an efficient estimator exists or that one can be found. Another consequence of this principle is that an efficient estimator extracts all the available information from the observations. Efficiency amounts to the extracted information being equal to the existing information.

4.1.1 The CRLB for standalone spherical positioning

When LBL positioning is used alone, without other complementary references, the precision of such a solution is based on (1) the precision of the range measurements, (2) the geometry of the fixed transponders and mobile host, (3) the accuracy of estimate of the speed of sound and (4) the uncertainty in the estimated location of the fixed seafloor transponders. We can

consider each of these sources of uncertainty by applying the CRLB framework to the spherical positioning measurement model described in Section 3.2. The range measurements are assembled into an measurement vector of length n.

$$\boldsymbol{Z}_r = \{z_{r_i}\} = \boldsymbol{h}(\boldsymbol{x}_h, \boldsymbol{x}_{\boldsymbol{b}_i}) + \boldsymbol{w}_r \tag{12}$$

where $\boldsymbol{h}(\ )$ is the non-linear function for spherical positioning (equation (1)) and $\boldsymbol{w}_r$ is a zero mean random vector with covariance $\boldsymbol{\Sigma}_{\mathrm{r}}$.

$$\boldsymbol{w}_r \sim \mathcal{N}(0, \boldsymbol{\Sigma}_{\mathrm{r}}) \tag{13}$$

The CRLB is calculated by linearizing the measurement model about an operating point, $\boldsymbol{x}_{h_o}$. The result is summarized by the first derivative of the measurement equation evaluated at the operating point, i.e., the Jacobian matrix $\boldsymbol{C}$. For the linearized measurement model with additive Gaussian noise, the CRLB is a matrix combination of the Jacobian, representing the current system geometry, and the measurement covariance quantifying the observation uncertainty.

$$\boldsymbol{\Lambda} = \boldsymbol{C}^{\boldsymbol{T}} {\boldsymbol{\Sigma}_{\mathrm{r}}}^{-1} \boldsymbol{C} \tag{14}$$

The CRLB is the best-case performance of an unbiased estimator designed to estimate the mobile host position based on uncertain range observations. The CRLB matrix is the minimum value of the covariance matrix for any unbiased estimate of position, i.e.,

$$\boldsymbol{\Lambda} \leqslant \boldsymbol{\Sigma}_{\mathrm{x_h}} = \boldsymbol{E}\left[[\hat{\boldsymbol{x}}_h - \overline{\boldsymbol{x}}_h][\hat{\boldsymbol{x}}_h - \overline{\boldsymbol{x}}_h]^T\right] \tag{15}$$

where $\overline{\boldsymbol{x}}_h$is the unknown true position of the host and $\hat{\boldsymbol{x}}_h$ is the estimated mobile host position. To summarize, the CRLB is a best-case estimate of the state covariance of the position solution as expressed in based on the geometry of the static acoustic beacons, the location of the host relative to the beacons and the range uncertainty.

4.1.2 The CRLB for combined odometry and positioning

The CRLB framework is also capable of analyzing the tradeoffs inherent in combining observations into an integrated navigation solution. In particular, we are interested in quantifying the tradeoffs involved in combining LBL absolute positioning with DVL dead-reckoning.

To apply the CRLB framework to this case requires a measurement model including both the high update rate odometry measurements of relative distance travelled and infrequent absolute position updates. In one-dimension the absolute position measurement uncertainty is equivalent to the range uncertainty (σ_r). To consider two-dimensional the odometry observation model from equations (7)-(9) we sum the two independent components of uncertainty. This simplification is similar to the notion of scalar horizontal precision discussed in the next section.

$$\sigma_o^2 = \mathrm{t}\,\sigma_v^2 + \mathrm{d}^2\,\sigma_\psi^2 \boldsymbol{\Lambda} \leqslant \boldsymbol{\Sigma}_{\mathrm{x_h}} = \boldsymbol{E}\left[[\hat{\boldsymbol{x}}_h - \overline{\boldsymbol{x}}_h][\hat{\boldsymbol{x}}_h - \overline{\boldsymbol{x}}_h]^T\right] \tag{16}$$

Now we can create a combined one-dimensional measurement model for a set of n absolute position updates with $n-1$ interspersed odometry measurements.

$$\boldsymbol{Z_c} = \begin{Bmatrix} \mathrm{x}_1 \\ \vdots \\ \mathrm{x}_\mathrm{n} \\ (\mathrm{x}_2 - \mathrm{x}_1) \\ \vdots \\ (\mathrm{x}_\mathrm{n} - \mathrm{x}_{\mathrm{n}-1}) \end{Bmatrix} + \boldsymbol{\omega}_\mathrm{c} \tag{17}$$

The additive noise vector, $\boldsymbol{\omega}_\mathrm{c}$, is modelled using a zero-mean Gaussian distribution. The individual measurements are considered to be independent, resulting in a covariance matrix that based on the standalone range measurements and odomentry measurements.

$$\omega_c \sim \mathcal{N}(0, \boldsymbol{\Sigma}_\mathrm{c}) \tag{18}$$

$$\boldsymbol{\Sigma}_\mathrm{c} = \begin{bmatrix} \sigma_r^2 \, \boldsymbol{I}_n & 0 \\ 0 & \sigma_o^2 \, \boldsymbol{I}_{n-1} \end{bmatrix} \tag{19}$$

Where $\boldsymbol{I}_n$is an $n \times n$ identity matrix.

4.2 Metrics for positioning performance

Horizontal dilution of precision (HDOP) and *circular error probable* (CEP) provide a quantifiable measure to succinctly convey the positioning precision for design and deployment decisions. The two positioning metrics are based the uncertainty in host (mobile station or vehicle) position estimate. The covariance matrix of the unknown error is the state estimate is

$$\boldsymbol{\Sigma}_{\mathbf{x}_\mathrm{h}} = \begin{bmatrix} \sigma_x^2 & \sigma_{xy}^2 & \sigma_{xz}^2 \\ \sigma_{xy}^2 & \sigma_y^2 & \sigma_{yz}^2 \\ \sigma_{xz}^2 & \sigma_{yz}^2 & \sigma_z^2 \end{bmatrix} \tag{20}$$

Because typical positioning geometries afford different performance in the horizontal plane as compared with the vertical dimension, the three-dimensional covariance is often decomposed into the horizontal (2D) and vertical components. The horizontal components (x and y) of the covariance represented an uncertainty ellipses as illustrated in Fig. 6.

4.2.1 Dilution of precision

Dilution of precision metrics are common in GPS applications. The horizontal dilution of precision comes directly from the Cartesian components (x and y) of the position estimate covariance matrix in equation (20).

$$\sigma_{hdop} = \frac{\sqrt{\sigma_x^2 + \sigma_y^2}}{\sigma_r} \tag{21}$$

The HDOP metric is normalized by the range uncertainty (σ_r)to isolate the sensitivity of the metric to the solutions geometry. Fig. 7 illustrates how this Cartesian interpretation overestimates the uncertainty by describing a rectangular boundary of uncertainty ellipse.

4.2.2 Circular error probable

In contrast to the DOP metric, the CEP metric is volumetric and non-normalized. The CEP defines the radius of the smallest circle, centered at the estimate, that has a 50% probability

of containing the true value. A linear approximation of the CEP can be derived from the estimate covariance.

$$CEP \approx 0.59\ (\sigma_L + \sigma_S) \tag{22}$$

where σ_L and σ_S are the major and minor axes of the uncertainty ellipse as shown in Fig. 7. The major and minor axes are the eigenvalues of the two-dimensional covariance matrix. The difference between the true CEP and the approximation of equation (22) is less than 1.5% when the uncertainty ellipse has a low aspect ratio ($0.5\sigma_L \leq \sigma_S \leq \sigma_L 0.5$), otherwise a quadratic approximation should be used (Nelson, 1988).
The CEP metric is volumetric because it uses the principle directions rather than the Cartesian directions, but is not normalized and therefore is a function of both the geometry and the range uncertainty.

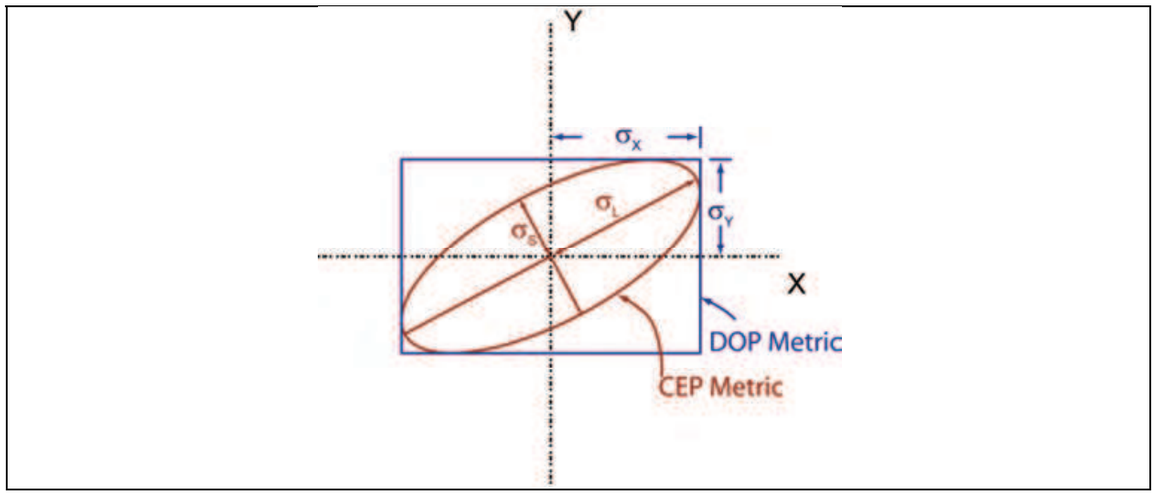

Fig. 7. Illustration of the covariance metrics. Geometrically the 2D covariance can be represented with an ellipse. The diagonal terms of the fully populated 2x2 matrix are σ_x^2 and σ_y^2. The square root of the two eigenvalues are one half major (σ_L) and minor (σ_S) axes of the ellipse. (Figure is adapted from (Kaplan, 1996).)

4.3 Results: Predicting performance metrics using the CRLB

Using the estimation framework of Section 4.1 and the performance metrics from Section 4.2 we can quantify the tradeoffs involved in designing standalone LBL positioning and integrated LBL/DVL navigation.

4.3.1 Standalone LBL configuration

Applying the CRLB to standalone LBL positioning enables the designer to predict the influence of transponder geometry, host location and range uncertainty on the LBL solution. Fig. 8 shows the results of this analysis. To generate these results the CRLB (equation (14)) is evaluated at each point in the two-dimensional space. The figure shows the results for a prototypical configuration, where the transponders are arranged in an equilateral triangle. The specific example shown in Fig. 8 illustrates the general process. This process has proven useful in deciding how to configure a LBL solution or deciding the level of range precision necessary to meet a particular performance specification.

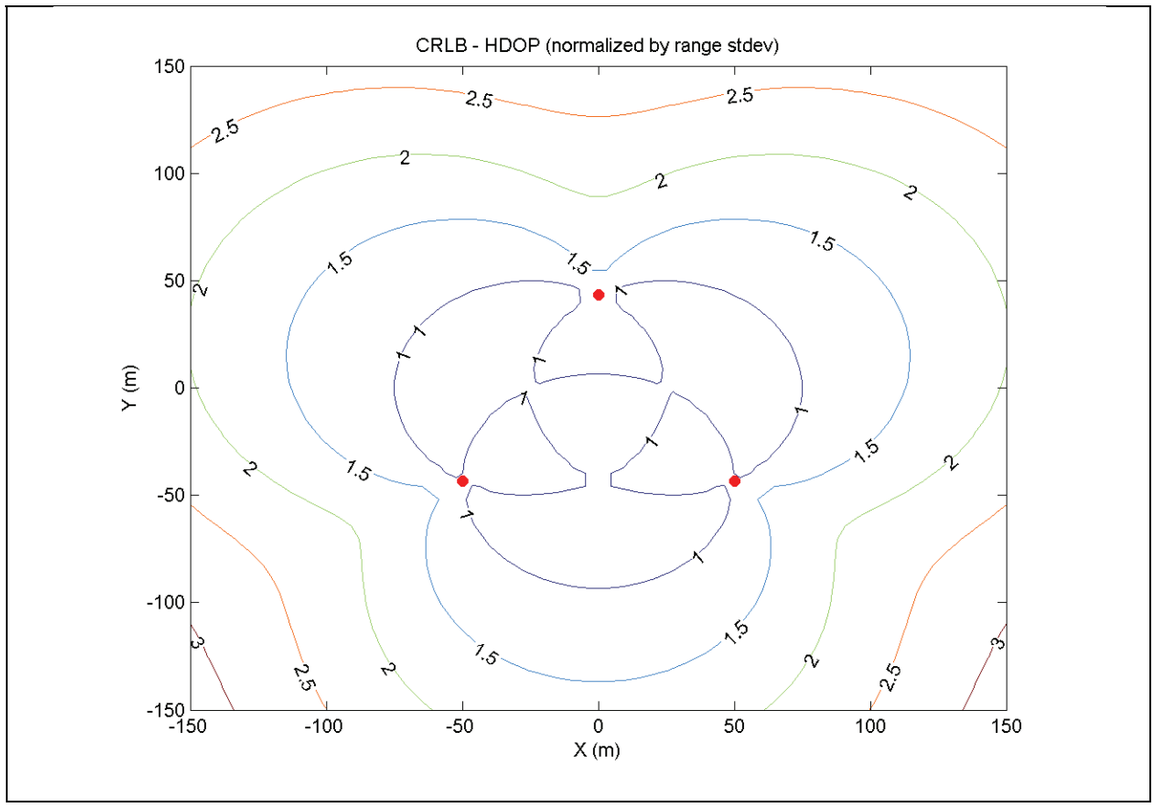

Fig. 8. Positioning performance prediction for standalone LBL positioning. The transponder locations are indicated by the red markers in an equilateral triangle near the origin. The contours show lines of constant HDOP.

4.3.2 Integrated LBL/DVL solution

Building on the standalone analysis of the previous section, next we use the CRLB framework to consider design decisions inherent in combining absolute positioning (LBL) and odometry dead-reckoning (DVL+Heading). The sensing modalities are best used in concert, where the two information sources can complement each other. The CRLB framework, using the measurement model in equation (17), quantifies the benefits of this combination.

The LBL and DVL sensing modalities must be matched to realize the potential of the complementary nature of these two navigation methods. Fig. 9 illustrates the constructive combination of LBL range observations, DVL velocity measurements and heading reference using a simple one-dimensional model. This comparison guides the selection of relative precision of the various sensors and the required update rate to leverage ability of absolute positioning to constrain the drift inherent to dead reckoning.

The two asymptotes in Fig. 9 are illustrative. On the right, in Region 3, we see that as odometry error is large, the overall positioning uncertainty is limited to be approximately equivalent to the absolute positioning uncertainty, indicated by $\sigma_o \,/\, \sigma_r \cong 1.0$ when the dead-reckoning uncertainty is greater than twice the absolute uncertainty ($\sigma_o > 2.0\,\sigma_r$). This could be caused by either high uncertainty in the velocity or heading measurements or large update times between absolute position updates. Conversely, the left side of the figure, Region 1, shows how precise odometry between absolute position updates links the sequential updates together. As the odometry becomes more precise the overall position

uncertainty approaches the bound of $\sigma_x = \sigma_r/\sqrt{N}$, where N is the number of discrete position updates (in this case $N = 100$). This limiting case represents perfect odometry, where the distance between absolute reference updates is known.

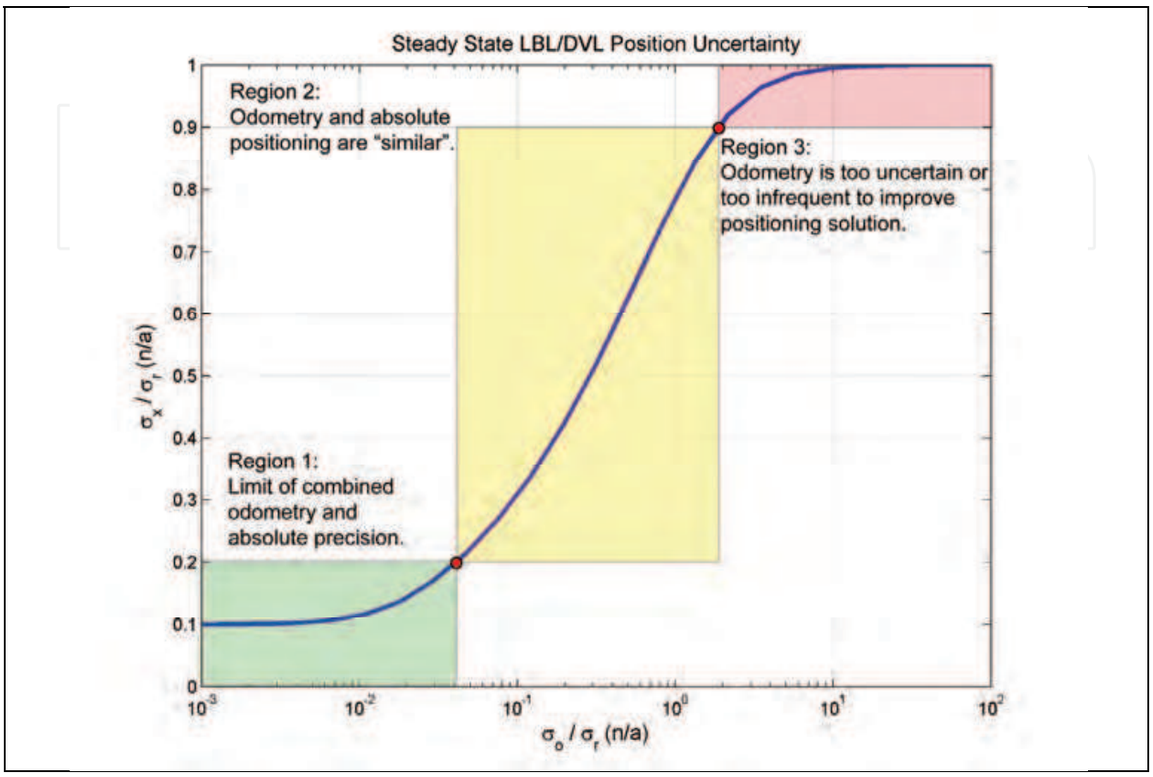

Fig. 9. Based on the one-dimensional model, this figure quantifies the tradeoffs in designing a complementary positioning solution using absolute positioning (LBL) and dead-reckoning odometry (DVL+Heading). The vertical axis shows position uncertainty (σ_x) normalized by the absolute reference uncertainty (σ_r). The horizontal axis shows the ratio of total odometry uncertainty (σ_o) to absolute reference uncertainty. Designing a solution in Region 1, with $\frac{\sigma_o}{\sigma_r} < 0.04$, successfully leverages the complementary nature of the two modes of navigation.

As an illustration we present an example using representative numbers for instruments typical on modern underwater platforms. Based on Fig. 9 we would like to design the positioning solution to operate in Region 1, where the total odometry uncertainty is less then 0.04 times the absolute positioning uncertainty, i.e.,

$$\sigma_o = \sigma_v \sqrt{t} + d\, \sigma_\psi < 0.1\, \sigma_r \tag{23}$$

Typical vehicle instrumentation might consist of an 1,200 kHz RDI DVL[3] ($\sigma_v = 3$ mm/s), an Octans true north heading reference[4] ($\sigma_\psi = 0.1$ degrees) and Benthos LBL transponders[5] ($\sigma_r \cong 3.0$ m). Furthermore we can assume a typical velocity of 1.0 m/s for the purposes of demonstration, resulting in $d = 1.0\, t$. Therefore,

[3] 1,200 kHz Workhourse Navigator Doppler velocity log by Teledyne RD Instruments.
[4] 6000 Series Transponders by Teledyne Benthos.
[5] Octans Fiber Optic Gyroscope (FOG) by Ixsea.

$$0.003\sqrt{t} + 0.0035\,t < 0.04\ (3.0) \tag{24}$$

Resulting in a required update rate of $t < 56$ seconds. Such an infrequent update rate is a consequence of the precision of the dead-reckoning solution.

5. Next steps: Opportunities to improve AUV navigation

Navigation continues to limit the application of AUV technology. As AUVs continue to be adopted by new users for new applications the fundamental navigation challenges must be addressed to further this expansion. Starting from the current state of the art we attempt to identify a few fruitful areas for continued research and development; areas that promise to have a strong impact on the design of new AUV systems.

5.1 Crossing chasms

There are gaps in current AUV navigation capabilities. Two of these gaps are explored below along with possible directions aimed at closing these gaps.

5.1.1 Decreasing transponder dependence

Many efforts in navigation research and development seek to reduce (or eliminate) the role of seafloor moored transponders in a navigation solution. As discussed above, LBL transponders provide an absolute reference, but this comes at a high cost. Transponders are deployed and surveyed from the surface in preparation for AUV missions and then recovered after completion of the mission. This evolution erodes operational efficiency, requiring hours or even days to complete depending on the environment and the mission. Such a seafloor-based external reference also limits the range of an AUV; typical transponder networks can only cover a few square kilometres.

Work has been done to eliminate the survey step in deploying transponders. One solution is to place the transponders at the surface, on floating buoys, where GPS can provide constant position updates. This has been used for tracking (the position is recorded at the surface, but not available subsea in real-time) AUVs for survey operations (Desset, Damus, Morash, & Bechaz, 2003). Another approach is to concurrently localize the fixed transponders while navigating using the range information. Using concurrent localization and mapping (CML), also known as simultaneous localization and mapping (SLAM), researchers have created a consistent map of the environment using only range information when the transponder locations are not known before the mission (Olson, Leonard, & Teller, 2006). Yet another approach is to have the AUV actually deploy the fixed transponders. This solution addresses a military need to limit the detection for AUV operations.

Instead of reducing the time spent on survey, another possible method is to decrease the number of transponders necessary to provide an absolute reference. Initial research efforts were focused on proving the theory of single beacon navigation (Larsen M. B., 2000). More recently this effort has moved from theoretical research to practical implementation, including algorithm development and integration into operational platforms such as the REMUS AUV (Hartsfield, 2005).

The incorporation of reliable acoustic communication has provided additional opportunity solutions to decrease the dependence on acoustic transponders. With the ability to transmit ephemeris data from a surface ship to the submerged platform, it becomes possible to eliminate the transponders all together and use the moving surface ship (with GPS navigation)

as fixed reference (Eustice, Whitcomb, Singh, & Grund, 2007). The Hugin AUV, a successful commercial survey tool, has used a similar technique to provide position updates and change the AUV mission from the surface (Vestgard, Storkersen, & Sortland, 1999)

5.1.2 Sensors: payload versus navigation

Current systems differentiate between navigation sensors and payload sensors. Navigation sensors are specifically for collecting measurements to position an AUV. These observations are processed in real-time using a variety of perception algorithms. In contrast, payload instruments collect data for future processing. Powerful instruments such a multibeam sonar, high quality still cameras, etc. are used to collect high resolution data about the environment, but this information is not used in real-time.

Many projects are seeking to alleviate this divide between payload and navigation sensors. Vision based algorithms promise to leverage the optical images to constrain the unbounded error growth for underwater applications (Huster & Rock, 2003) (Eustice, Pizarro, & Singh, 2004). Similarly, combining course navigation with bathymetry can serve to improve both the positioning and final data product (Roman & Singh, 2006). Many researchers have developed estimation techniques that make use of the bathymetry. These terrain based methods make use of either a fathometer or bathymetric sonar to position the vehicle relative to a known (or partially unknown) map of the seafloor (Tuohy, Leonard, Bellingham, Patrikalakis, & Chryssostomidis, 1996) (Williams, Dissanayake, & Durrant-Whyte, 1999). Each of these techniques offers a path toward crossing the artificial divide between payload sensors and navigation aids.

5.2 Operations in challenging environments

The application of AUV technology for exploration and investigation is moving into new environments. This valuable technology has improved our ability to accomplish nearbottom surveys in the open ocean. Now the needs of new users are necessitating adaptation of AUV technologies to a variety of interesting and challenging underwater environments. Under-ice missions promise to open the important polar regions to the observational power of autonomous platforms (Kunz, et al., 2008) (McEwen, Thomas, Weber, & Psota, 2005). Obviously navigation under-ice is very important to the safety of such mission; the AUV must be able to return a safe region for recovery. Possibly not so obvious are the challenges presented by the acoustics of under-ice environments. The upward refracting acoustic environment can create shadow zones, restricting the means of communication and positioning. Furthermore the ice cover can shift at significant speeds relative to the seafloor, creating dynamic environment for navigation (von der Heydt, Duckworth, & Baggeroer, 1985) (Deffenbaugh, Schmidt, & Bellingham, 1993).

Another environment that presents new challenges for AUV operations is coastal zones. The littoral zone has been recognized by military users as a key new frontier for operations. Similarly, environmental assessment of shallow marine environments (e.g., coral reefs) is pushing AUV missions towards the coast. From a navigation perspective, these shallow water environments can be more dynamic than the deep ocean with increased multipath and high background noise from breaking waves and other disturbances.

A last example of new environments for AUV operations is the exploration of freshwater caves, cenotes, using novel AUVs. Research expeditions have used three dimensional SLAM-based to map these underwater caves. Interestingly, these expeditions are supported by resources for space exploration because of the analogy between cenote exploration and the environment operators anticipate for autonomous exploration of other planets (Kumagni, 2007).

6. Continued improvement in AUV navigation

One way to set expectations for the future is to look at the past. In the past two decades of AUV platform development autonomous navigation has provided fundamental supporting technology through new instruments, new algorithms and new methods of operation. As AUV platforms continue to proliferate, becoming commercially available to a wider user base, we can expect the opportunities for improved navigation methods to similarly expand. Operators and vehicle designers will need new solutions that increase efficiency, decrease cost and allow for the application of AUV technology to exciting new environments.

7. Acknowledgements

The Deep Submergence Lab at Woods Hole Oceanographic provided the data and images used in developing the illustrations in Fig. 2 and Fig. 3. Also, Joel Gendron illustrated Fig. 4. The publication of this chapter was supported by the Franklin W. Olin College of Engineering in Needham, Massachusetts.

8. References

Bar-Shalom, Y., Li, X. -R., & Kirubarajan, T. (2001). *Estimation with applications to tracking and navigation.* John Wiley and Sons, Inc.

Bingham, B., Mindell, D., Wilcox, T., & Bowen, A. (2006). Integrating precision relative positioning into JASON/MEDEA ROV operations. *Marine Technology Society (MTS) Journal, 40* (1), pp. 87-96.

Catipovic, J. A. (1990). Performance limitations in underwater acoustic telemetry. *IEEE Journal of Oceanic Engineering, 15* (3), pp. 205-216.

Deffenbaugh, M., Schmidt, H., & Bellingham, J. G. (1993). Acoustic navigation for Arctic under-ice AUV missions. *OCEANS '93. Proceedings.*

Desset, S., Damus, R., Morash, J., & Bechaz, C. (2003). Use of GIBs in AUVs for underwater archaeology. *Sea Technology*.

Dunlap, G. D. (1975). *Dutton's Navigation and Piloting.* Unites States Naval Institute Press.

Eustice, R. M., Singh, H., & Leonard, J. J. (2006). Exactly sparce delayed-state filters for view-based SLAM. *IEEE Transactions on Robotics, 22* (6), pp. 1100-1114.

Eustice, R. M., Whitcomb, L. L., Singh, H., & Grund, M. (2007). Experimental results in synchronous-clock one-way-travel-time acoustic navigation for autonomous underwater vehicles. *Proc. of the IEEE International Conference on Robotics and Automation*, 4257-4264.

Eustice, R., Pizarro, O., & Singh, H. (2004). Visually augmented navigation in an unstructured environment using a delayed state history. *Proc. of the IEEE International Conference on Robotics and Automation, 1*, 25-32.

Frew, E. W., & Rock, S. M. (2003). Trajectory generation for monocular-vision based tracking of a constant-velocity target. *Proc. of the IEEE International Conference on Robotics and Automation.* Taipei, Taiwan.

Hartsfield, J. C. (2005). *Single Transponder Range Only Navigation Geometry (STRONG) Applied to REMUS Autonomous Under Water Vehicles.* Masters Thesis, Massachusetts Institute of Technology and Woods Hole Oceanographic Institution.

Hunt, M. M., Marquet, W. M., Moller, D. A., Peal, K. R., Smith, W. K., & Spindel, R. C. (1974). *An acoustic navigation system.* Technical Report WHOI-74-6, Woods Hole Oceanographic Institution.

Huster, A., & Rock, S. M. (2003). Relative position sensing by fusing monocular vision and inertial rate sensors. *Proc. of the 11th International Conference on Advanced Robotics*, *3*, pp. 1562-1567. Coimbra, Portugal.

Huster, A., Fleischer, S. D., & Rock, S. M. (1998). Demonstration of a vision-based dead-reckoning system for navigation of an underwater vehicle. *Proc. of the MTS/IEEE Oceans Conference*, (pp. 326-330).

Kaplan, D. (1996). *Understanding GPS.* Artech House Publisher.

Kinsey, J. C., Smallwood, D. A., & Whitcomb, L. L. (2003). A new hydrodynamics test facility for UUV dynamics and control research. *Proc. of the MTS/IEEE Oceans Conference.* San Diego, CA.

Kumagni, J. (2007). Swimming to Europa. *Spectrum, IEEE , 44* (9), pp. 33-40.

Kunz, C., Murphy, C., Camilli, R., Sing, H., Bailey, J., Eustice, R., et al. (2008). Deep sea underwater robotic exploration in the ice-covered Arctic ocean with AUVs. Proc. of *IEEE/RSJ International Conference on Intelligent Robots and Systems*, (pp. 3654-3660).

Larsen, M. B. (2000). High performance Doppler-inertial navigation - experimental results. *Proc. of the MTS/IEEE Oceans Conference.*

Larsen, M. B. (2000). Synthetic long baseline navigation of underwater vehicles. *Proc. of the MTS/IEEE Oceans Conference*, *3*, pp. 2043-2050.

McEwen, R., Thomas, H., Weber, D., & Psota, F. (2005). Performance of an AUV navigation system at Arctic latitudes. *IEEE Journal of Oceanic Engineering, 30* (2), pp. 443-454.

Milne, P. H. (1983). *Underwater Acoustic Positioning Systems.* Houston: Gulf Publishing Company.

Nelson, W. (1988). *Use of circular error probability in target detection.* United States Air Force Hanscom Air Force Base: MITRE Corporation.

Olson, E., Leonard, J. J., & Teller, S. (2006). Robust range-only beacon localization. *IEEE Journal of Oceanic Engineering, 31* (4), pp. 949-958.

Roman, C., & Singh, H. (2006). Consistency based error evaluation for deep sea bathymetric mapping with robotic vehicles. *Proc. of IEEE International Conference on Robotics and Automation*, pp. 3569-3574.

Smith, S. M., & Kronen, D. (1997). Experimental results of an inexpensive short baseline acoustic positioning system for AUV navigation. *Proc. of the MTS/IEEE Oceans Conference, 1*, pp. 714-720.

Tuohy, S. T., Leonard, J. J., Bellingham, J. G., Patrikalakis, N. M., & Chryssostomidis, C. (1996). Map based navigation for autonomous underwater vehicles. *International Journal of Offshore and Polar Engineering*.

Vestgard, K., Storkersen, N., & Sortland, J. (1999). Seabed surveying with Hugin AUV. *Proc. of the 11th International Symposium on Unmanned Untethered Submersible Technology.* Durham, NH.

von der Heydt, K., Duckworth, G., & Baggeroer, A. (1985). Acoustic array sensor tracking system. *Proc. of the MTS/IEEE Oceans Conference, 17*, pp. 464-471.

Whitcomb, L. L., Yoerger, D. R., & Singh, H. (1999). Combined Doppler/LBL based navigation of underwater vehicles. *Proc. Int. Symp. on Unmanned Untethered Submersible Technology.*

Williams, S. B., Dissanayake, G., & Durrant-Whyte, H. (1999). Towards terrain-aided navigation for underwater robotics. *Advanced Robotics, 15* (5), pp. 533-549.

Underwater Vehicles

Edited by Alexander V. Inzartsev

ISBN 978-953-7619-49-7

Hard cover, 582 pages

Publisher InTech

Published online 01, January, 2009

Published in print edition January, 2009

For the latest twenty to thirty years, a significant number of AUVs has been created for the solving of wide spectrum of scientific and applied tasks of ocean development and research. For the short time period the AUVs have shown the efficiency at performance of complex search and inspection works and opened a number of new important applications. Initially the information about AUVs had mainly review-advertising character but now more attention is paid to practical achievements, problems and systems technologies. AUVs are losing their prototype status and have become a fully operational, reliable and effective tool and modern multi-purpose AUVs represent the new class of underwater robotic objects with inherent tasks and practical applications, particular features of technology, systems structure and functional properties.

InTech Europe
University Campus STeP Ri
Slavka Krautzeka 83/A
51000 Rijeka, Croatia
Phone: +385 (51) 770 447
Fax: +385 (51) 686 166
www.intechopen.com

InTech China
Unit 405, Office Block, Hotel Equatorial Shanghai
No.65, Yan An Road (West), Shanghai, 200040, China
中国上海市延安西路65号上海国际贵都大饭店办公楼405单元
Phone: +86-21-62489820
Fax: +86-21-62489821

IntechOpen